



Highly dispersed Rh-, Pt-, Ru/Ce_{0.75}Zr_{0.25}O_{2-δ} catalysts prepared by sorption-hydrolytic deposition for diesel fuel reforming to syngas



T.B. Shoyukhorova^a, P.A. Simonov^{a,c}, D.I. Potemkin^{a,b}, P.V. Snytnikov^{a,b,c,*}, V.D. Belyaev^{a,b,c}, A.V. Ishchenko^{a,b}, D.A. Svintsitskiy^{a,b}, V.A. Sobyanin^{a,*}

^a Boreskov Institute of Catalysis, Pr. Akademika Lavrentieva, 5, Novosibirsk, 630090, Russia

^b Novosibirsk State University, Pirogova St., 2, Novosibirsk, 630090, Russia

^c UNICAT Ltd, Pr. Akademika Lavrentieva, 5, Novosibirsk, 630090, Russia

ARTICLE INFO

Keywords:

Diesel autothermal reforming
Steam conversion of hexadecane
Hydrogen-rich stream
Syngas
Rhodium catalysts
Ceria-zirconia

ABSTRACT

Three noble metal catalysts (Rh-, Pt-, Ru/Ce_{0.75}Zr_{0.25}O_{2-δ}) for reforming of hydrocarbons were studied in steam and autothermal process conditions. Each catalyst was prepared by sorption-hydrolytic deposition with a metal loading of 0.1 mmol/g. The main idea of this technical approach was to form a solution of “metal complex + alkaline agent” that was metastable at given conditions (temperature, concentrations) with respect to homogeneous metal hydroxide precipitation, due to the kinetic inertness of the metal complexes for ligand exchange. As the support surface accelerated heterogeneous nucleation and growth of metal hydroxide particles, addition of the support to the reagent mixture initiated the hydrolysis which led to uniform depositing of 1–2 nm metal particles over the support surface. The Rh-based catalyst synthesized surpassed the Ru- and Pt-based catalysts in activity and stability in that under the experimental conditions, complete *n*-hexadecane conversion and equilibrium reformate product distribution were observed for 1-wt. % Rh/Ce_{0.75}Zr_{0.25}O_{2-δ} for 17 h. This catalyst also showed competitive performance in autothermal reforming of diesel fuel providing stable operation for 9 h.

1. Introduction

In recent decades, the development of new technologies for on-site power generation has attracted considerable attention [1,2]. Among commercially available auxiliary power units of 1-kW scale, solid oxide fuel cell (SOFC) based systems are considered as the most effective for electricity generation. Compared with thermoelectric, gasoline and diesel generators, SOFC-based systems of similar mass and volume demonstrate higher efficiency, along with silent and reliable operation.

Diesel fuel is an attractive source of hydrocarbons due to its high energy density, widespread availability and mature distribution infrastructure. In recent years, a number of papers have been published on studies of steam and autothermal reforming, and partial oxidation of diesel fuel to produce hydrogen gas for SOFC operation [3–13]. Being a complex blend of C₁₀–C₂₄ hydrocarbons, including aromatic compounds, diesel fuel is difficult to reform into syngas, because of accompanying side reactions resulting in undesired coke formation. The latter results from both catalytic and homogeneous thermocracking reactions that produce light hydrocarbons, such as ethylene, easily converted to carbon [14–16].

To avoid undesirable homogeneous non-catalytic reactions, numerous engineering solutions have been proposed, including various types of injectors, ultrasonic atomizers, and special evaporation and mixing chambers for homogenizing the reaction mixture prior to the catalytic process [15–17]. Catalysts shaped in ceramic or metallic honeycomb blocks, foams, wire meshes, or microchannel plates supporting an active component layer provide low pressure drop and effective heat and mass transfer. Numerous types of catalysts have been studied to improve the performance of diesel reforming. Rh, Ru, Pt and Ni, their bimetallic compositions together with various transition metals supported on individual or mixed Zr-, Ce-, Gd-, La-, and Al-oxides have been designed as active catalyst components. Perovskite and pyrochlore structures have also been widely studied [20–27]. Among others, precious metals on ion-conducting supports have shown the highest activity, stability and, therefore, durability in diesel reforming. In addition to carbon deposition, catalyst deactivation may be caused by sintering of the supported metal particles at the high temperatures of the diesel reforming process, resulting in a decreased reforming rate for the slow-reacting diesel components, such as aromatic compounds, promoting coke formation and further accelerating catalyst

* Corresponding authors at: Boreskov Institute of Catalysis, Pr. Akademika Lavrentieva, 5, Novosibirsk, 630090, Russia.
E-mail addresses: pvsnyt@catalysis.ru (P.V. Snytnikov), sobyanin@catalysis.ru (V.A. Sobyanin).

deactivation.

Ion-conducting oxide supports for diesel reforming catalysts usually have low specific surface area making the deposition of the required amount of highly dispersed metal particles difficult using currently available preparation techniques (e.g. adsorption, impregnation, incipient wetness impregnation, and deposition-precipitation). The problem is especially complex for wire mesh, foam or honeycomb supports, resulting in insufficiently high reforming activity and durability.

In this paper, composite oxide $\text{Ce}_{0.75}\text{Zr}_{0.25}\text{O}_{2-\delta}$ supported Rh, Ru and Pt catalysts synthesized using a novel preparation technique were studied for steam reforming (SR) of *n*-hexadecane (HD) used as a diesel surrogate, and autothermal reforming (ATR) of HD and conventional diesel fuel, the type of “summer” Euro-5 (SD). The catalytic activity was tested using a micro-reactor setup. Transmission Electron Microscopy (TEM), BET, temperature-programmed oxidation (TPO), X-ray photoelectron spectroscopy (XPS) and CO chemisorption techniques were used for catalyst characterization and coke formation studies.

2. Experimental

2.1. Catalyst preparation

Composite oxide $\text{Ce}_{0.75}\text{Zr}_{0.25}\text{O}_{2-\delta}$ (CZ) was purchased from Eccoalliance Ltd. (Russia), prepared by direct precipitation as described in detail elsewhere [28]. Solutions of Ce^{3+} and ZrO^{2+} nitrates were combined in fixed proportions resulting in concentrations of components totaling 0.1 g cm^{-3} . The composite oxide was precipitated from the solution by adding 25% aqueous ammonia dropwise under permanent stirring. The mixture was held at 100°C and atmospheric pressure for 120 h. Thereafter, the precipitate was filtered and repulped in isopropanol. The resulting slurry was dried at 100°C for 12 h and calcined at 500°C for 2 h, and then at 800°C for 1 h. The synthesized CZ material was crushed in an agate mortar with the 0.2–0.5 mm fraction separated for further catalyst synthesis. The CZ BET surface area was $69 \text{ m}^2 \text{ g}^{-1}$.

Catalysts were prepared by sorption-hydrolytic deposition as described in [29] that contained Pt, Ru and Rh deposited on CZ particles in the amount of 0.1 mmol/g (1 wt.% Ru and Rh, 1.9 wt.% Pt), denoted further as Ru/CZ, Rh/CZ and Pt/CZ, respectively. The main idea of this technical approach is to form a solution of “metal complex + alkaline agent” which is metastable at given conditions (temperature, concentrations) in respect to homogeneous metal hydroxide precipitation. This is due to the kinetic inertness of the metal complexes for ligand exchange [30]. As the support surface accelerates heterogeneous nucleation and growth of metal hydroxide particles [31], addition of a support to the reagent mixture initiates hydrolysis which leads to uniform depositing of the metals over the support surface.

For this purpose, a solution of metal chloride (RuCl_3 , RhCl_3 or H_2PtCl_4) was mixed with Na_2CO_3 in a molar ratio of $\text{Na}/\text{Cl} = 1$. The mixture was then brought into contact with the aqueous suspension of the CZ support. The deposition was performed at 5 °C for Pt, 60 °C for Ru and 75 °C for Rh. After the end of the deposition procedure (i.e., when no reaction of the solution with NaBH_4 was observed), the samples were thoroughly rinsed with hot water by decanting, dried and reduced in hydrogen flow at 250 °C for 30 min. The BET specific surface area of the prepared catalysts was close to that of the CZ support ($69 \text{ m}^2 \text{ g}^{-1}$).

For comparison purpose, 1 wt.%Rh supported on CZ was prepared by typical incipient wetness impregnation technique. This catalyst is further denoted as Rh/CZ(WI).

2.2. Catalyst characterization

The BET specific surface area (S_{BET}) of the support, as-prepared and used catalysts was determined from the complete nitrogen adsorption isotherms at -196°C using an ASAP 2400 sorptometer (Micromeritics,

USA).

The dispersion of the metal particles supported on the CZ, their specific surface area and mean size were evaluated using pulse chemisorption of CO in H_2 at 20°C . Prior to the CO chemisorption measurements, the catalysts were reduced in a hydrogen flow at 350°C for 30 min. The technique of pulse titration of the metal surface was adopted from [32,33].

The X-ray diffraction (XRD) patterns were obtained on a diffractometer X'tra (Thermo Scientific, Switzerland) using monochromatic $\text{CuK}\alpha$ radiation ($\lambda = 154.18 \text{ pm}$). The measurements were carried out in the 2θ range of 15 – 80° with a step of 0.05° and 5.0 s sampling time. The ICDD PDF-2 database was used for the phase composition analysis. The Rietveld refinement with quantitative phase analysis was performed using TOPAS v4.3 software. The sizes of the coherent scattering regions (D_{XRD}) were calculated by line broadening analysis according to the Scherrer equation.

To quantify the carbon formation during steam reforming of HD and autothermal reforming of SD, the used catalysts were studied by TPO using a TG209 F1 LibraThermo microbalance instrument (Netzsch, Germany). The feed gas, 0.6 vol. % O_2 in He , flowed at $70 \text{ cm}^3 \text{ min}^{-1}$. The temperature was raised linearly from 30 to 900°C at a rate of $10^\circ\text{C min}^{-1}$. The outlet CO_2 concentration was monitored on-line using a QMC-200 mass-spectrometer (Stanford Research Systems, USA).

X-ray photoelectron spectroscopy (XPS) was applied to determine surface composition of the as-prepared and used catalysts. The XPS measurements were carried out using an ES-300 photoelectron spectrometer (KRATOS Analytical, U.K.) with $\text{MgK}\alpha$ irradiation. Before the measurements, the catalyst samples were reduced at 250°C in H_2 (667 Pa) for 2 h in the preparation chamber of the spectrometer. The power of the X-ray was no more than 80 W to avoid X-ray damage of the catalyst surface. The spectra were calibrated by $\text{Ce}3d \text{ U''}$ line with binding energy of 916.7 eV . The XP spectra were processed with a proprietary in-house XPS-Calc program, which has been tested on a number of systems [34,35]. The Shirley-model was used for subtraction of the inelastic photoelectron background. The spectra were fitted by Gauss–Lorentz or Doniach–Sunjic functions.

The transmission electron microscopy (TEM) images of the as-prepared and used catalysts were obtained using a JEOL JEM 2010 electron microscope with 1.4 \AA resolution at 200 kV (JEOL Ltd., Japan). The interplanar spacing was analyzed, and the particles composition was determined using the JCPDS-ICDD database.

Detailed characterization by XPS and TEM was performed only for the Rh/CZ catalyst which had superior catalytic performance, as discussed in Sections 3.2–3.4, below.

2.3. Catalytic activity measurements

The reactions of *n*-hexadecane (Komponent-Reaktiv LLC, Russia) steam reforming, autothermal reforming of HD and SD were performed in a fixed-bed continuous-flow U-shaped quartz reactor (ID: 7 mm, catalyst bed length: 12 mm) at atmospheric pressure in the temperature range of 550 – 650°C . In all the experiments, 0.5 g of the catalyst was placed in the reactor together with a 50 mm piece of copper foam at the reactor inlet used as an evaporator at 450°C . The 130 mm space between the evaporator and the catalyst bed was filled with 1–2 mm quartz pellets homogenizing the reactants mixture. The fuels were fed via a capillary into the evaporator. The evaporated water from a steam generator together with the nitrogen carrier gas was supplied via a heated capillary to the evaporator and mixed with the vaporized fuel. Air was fed via a coaxially positioned capillary close to the catalyst bed. The reaction temperature was measured by a K-type thermocouple in the middle of the catalyst bed.

Prior to the experiment, the catalyst was reduced inside the reactor in a mixture of 10 vol. % H_2 in Ar at a heating rate of 6°C min^{-1} up to 600°C . The temperature was then changed to 550 or 650°C , and the reaction mixtures were fed to the reactor. The mixture compositions

Table 1

Specification of Euro-5 summer-grade diesel fuel used in the ATR experiments.

Parameter	Value
Monoaromatics	16.6 wt.%
Diaromatics	2.9 wt.%
Polyaromatics	0.26 wt.%
Paraffins (n- + iso-), Cycloparaffins	the rest
Sulfur content	8 ppm (w)
Nitrogen content	32 ppm(w)
Min. boiling point	195 °C
Dist. 95% evap.	350 °C
Density at T = 23 °C:	841 kg/m ³

were set respectively for each of the processes studied as follows:

- steam reforming: HD 1.6 g h⁻¹, H₂O 6 g h⁻¹; N₂ 1800 cm³ h⁻¹ making the ratio H₂O/C = 3 at the gas hour space velocity (GHSV) of 23,000 h⁻¹;
- autothermal reforming: HD or SD 1.7 g h⁻¹, H₂O 5.3 g h⁻¹, air 6000 cm³ h⁻¹ making the ratios H₂O/C = 2.5, O₂/C = 0.5 at GHSV of 30,000 h⁻¹.

Commercially available Euro-5 summer-grade diesel fuel was used in the experiments (see **Table 1** for fuel specifications).

Each experimental run was repeated three times. The results were well reproduced.

The reformates were analyzed using a GC-1000 gas chromatograph (Chromos, Russia) equipped with a thermal conductivity detector (TCD) and a flame ionization detector (FID) with methanator. Before analysis, water was removed from the reformate using a moisture trap. Concentrations of H₂ and N₂ separated in a CaA column with an Ar carrier gas were determined with TCD. The CO, CO₂, CH₄, and C₂–C₅ hydrocarbons were separated in a Chromosorb 106 column and quantified using FID. Conversion of HD and SD was determined gravimetrically every hour by collecting unreacted HD or SD at the reactor condenser. It was calculated by the following equation:

$$\text{Conversion (\%)} = \frac{V_0 \cdot t - m_1}{V_0 \cdot t} \cdot 100,$$

where V₀ is the inlet mass flow of HD or SD (g h⁻¹), t is the time of probe collecting (h), m₁ is the probe weight of unreacted HD or SD (g), respectively.

Thermodynamic equilibrium compositions of HD steam and auto-thermal reforming were calculated using HSC Chemistry software 7.0 and were used as reference data for interpreting the experimental results.

3. Results and discussion

3.1. Catalyst characterization

The XRD patterns of the CZ support, as-prepared and used catalysts contain peaks assigned to the fluorite-type solid solution Ce_xZr_{1-x}O_{2-δ} phase. For all samples, similar crystallite particle size (D = 110 Å) and unit cell parameter (a = 5.388 Å) were determined. No peaks related to metallic phases were identified due to the low concentration of the species.

According to CO chemisorption data, the average size of metal particles in the as-prepared Rh/CZ, Rh/CZ(WI), Ru/CZ and Pt/CZ catalysts was 1.1, 2.4, 1.2 and 1.8 nm, respectively. After HD SR experiments, slight agglomeration of the supported metal particles was observed. These data agree well with the TEM results exemplified by images of as-prepared (**Fig. 1a**) and used (**Fig. 1b**) Rh/CZ catalysts. The results show that CZ crystallites of 10–20 nm size form large porous aggregates of micron scale. The typical interplanar spacing for ceria and

zirconia of {111} and {200} planes varies within d = 3.03–3.20 Å and d = 2.65–2.72 Å, respectively, which proves formation of solid solutions of variable compositions. In the as-prepared catalyst, the Rh particles exist on the support surface predominantly in the form of 1–2 nm clusters. Some 3–4 nm particles with interplanar distances d = 2.196 Å and d = 1.902 Å corresponding to {111} and {200} planes, respectively, were observed as well.

After SD ATR experiments, the support crystallites increased in size to 20–30 nm, while the aggregate size remained the same. Additionally, carbon species in the form of 1–2 graphite layers appeared occasionally on the surface (**Fig. 1b**). The size of Rh particles increased slightly to 2–4 nm. After oxidative treatment of the catalyst, the carbon deposits disappeared, while the size of support crystallites and Rh particles remained unchanged.

The TEM results of as-prepared and used Rh/CZ(WI) catalysts demonstrated that the most part of Rh particles had the size of 2–4 nm.

Detailed XPS analysis of the as-prepared and used Rh/CZ samples preliminary reduced in the spectrometer was in line with the above observations. The obtained spectra of both samples were similar. However, the amount of surface carbon increased from 24 to 32 at.% for the used Rh/CZ catalyst. The increased intensity of C1s line at 285 eV, which can be attributed to graphite-like carbon [36,37], most likely indicates coking of the catalyst surface. The Zr3d XPS spectra of both samples (**Fig. 2a**) were reliably curve-fitted by one doublet component with E_b(Zr3d_{5/2}) ~182 eV, which corresponds to Zr⁴⁺ state in the oxide matrix [37,38]. The Ce3d spectrum (**Fig. 2b**) was split into several components corresponding to Ce³⁺ and Ce⁴⁺ states. In both samples, the content of Ce³⁺ ions was close to ~50%, indicating a deep reduction of the catalyst surface during interaction with hydrogen. The Rh3d XPS spectra (**Fig. 2c**) showed the maximum Rh3d_{5/2} peak at 307.2 eV corresponding to metallic rhodium [36–38]. Thus, notwithstanding the strong metal-support interaction in Rh-Ce_xZr_{1-x}O_{2-δ} [39], rhodium under these reaction conditions (reduction medium) most likely exists in a metallic state.

Temperature-programmed oxidation analysis showed Pt/CZ to be the most susceptible to coking: it accumulated 2.2 wt. % of carbon for 3 h of HD SR, while Ru/CZ – 1.2 wt. % for 8 h. Rh/CZ appears to be the most coking-resistant. It contained only 1.2 wt. % of carbon after 20 h operation in HD SR, and was almost coke-free (0.15 wt. % of carbon) after 18 h in a subsequent run at the HD and SD ATR conditions. For more details see Supplementary information, Fig. S2. Thus, the structure of highly dispersed Rh/CZ, Pt/CZ and Ru/CZ catalysts prepared by sorption-hydrolytic deposition technique was stable under the reaction conditions of HD SR and SD ATR.

3.2. Steam reforming of n-hexadecane

Fig. 3 illustrates the effect of time on stream on HD conversion and gas product distribution for HD SR over the Pt/CZ, Ru/CZ and Rh/CZ catalysts in a continuous-flow reactor.

The results show that Pt/CZ demonstrated the worst HD SR performance. At 550 °C, complete HD conversion was not reached, and during 3 h the conversion decreased from 59 to 27%. The concentrations of H₂, CO₂, CO and CH₄ (data not shown) decreased during the experiment, vol. %, from 52 to 24, from 16 to 7, from 2 to 0.2, and from 0.4 to 0.1, respectively. Total outlet concentration of C₂–C₅ hydrocarbons did not exceed 0.2 vol. %, and increased slightly with decreasing HD conversion.

During the first 5 h on stream, Ru/CZ provided complete HD conversion. The product distribution (H₂, CO₂, CO and CH₄) was close to the calculated equilibrium data. Only traces of outlet C₂–C₅ hydrocarbons were detected. However, for the next 3 h, the catalyst rapidly lost its activity: HD conversion dropped down to 46%, the outlet concentrations of H₂, CO₂, CO and CH₄ decreased to 41, 13, 1 and 0.1 vol. %, respectively.

Fig. 3 illustrates that Rh/CZ demonstrated stable operation for 8 h at

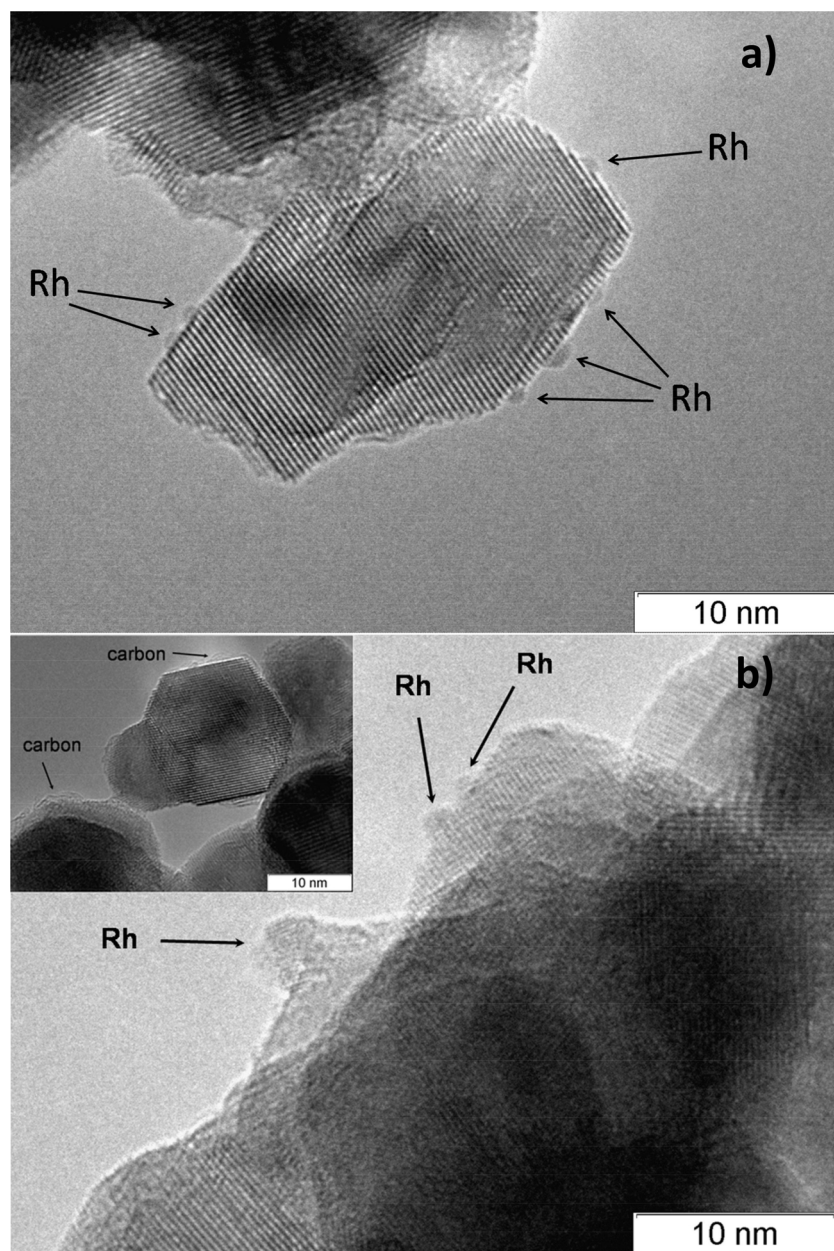


Fig. 1. TEM images of 1 wt.% Rh/CZ: (a) as-prepared and (b) used in SD ATR.

550 °C. It provided 100% conversion of HD with H₂-rich outlet mixture, vol. %: 54 H₂, 18 CO₂, 5 CO and ~6 CH₄ approximating the equilibrium composition. The catalyst was cooled to room temperature after the experiment and the HD SR was repeated at a higher temperature of 650 °C. For this purpose, the catalyst was reduced in a flow of 10 vol. % H₂ in Ar at 650 °C and then the reaction mixture was supplied to the reactor. Under these conditions, the catalyst remained stable for another 5 h providing 100% conversion of HD. The reformate product distribution differed from that observed at 550 °C corresponding to the equilibrium values calculated for 650 °C. Compared to HD SR at 550 °C, the H₂ and CO outlet concentrations increased to 61 and 7.5 vol. %, respectively, while the CO₂ and CH₄ concentrations decreased to 16 and 0.6 vol. %, respectively. Among C₂–C₅ hydrocarbons, pentane dominated; its concentration remained below 0.3 vol. % during the entire duration of the experiment. This most likely explains the slight deviation of the primary reaction product concentrations from the equilibrium composition.

Compared to the Rh/CZ catalyst prepared by sorption-hydrolytic

deposition, the Rh/CZ(WI) catalyst prepared by incipient wetness impregnation was much less stable under the same experimental conditions. (For more details see Supplementary information, Fig. S3). It provided a 100% conversion of HD at 550 °C for 4 h, but lost activity during the next 11 h: HD conversion dropped down to 85%, the outlet concentrations of H₂, CO₂, CO and CH₄ changed to 59, 17, 6 and 0.3 vol. %, respectively. The total concentration of C₂–C₅ hydrocarbons slightly increased with decreasing HD conversion, but remained below 0.2 vol. % during the entire duration of the experiment.

Thus, the activity and stability of the catalysts tested decreased in the order Rh/CZ > Ru/CZ > Pt/CZ. A similar sequence was observed in SR of methane [40,41], where the experimentally observed order of the metals intrinsic activity (Rh ~ Ru > Ni ~ Ir ~ Pt ~ Pd) was confirmed by density functional theory (DFT) calculations. Hence, Rh/CZ catalyst was selected for testing in the diesel ATR experiments and detailed characterization (Section 3.1).

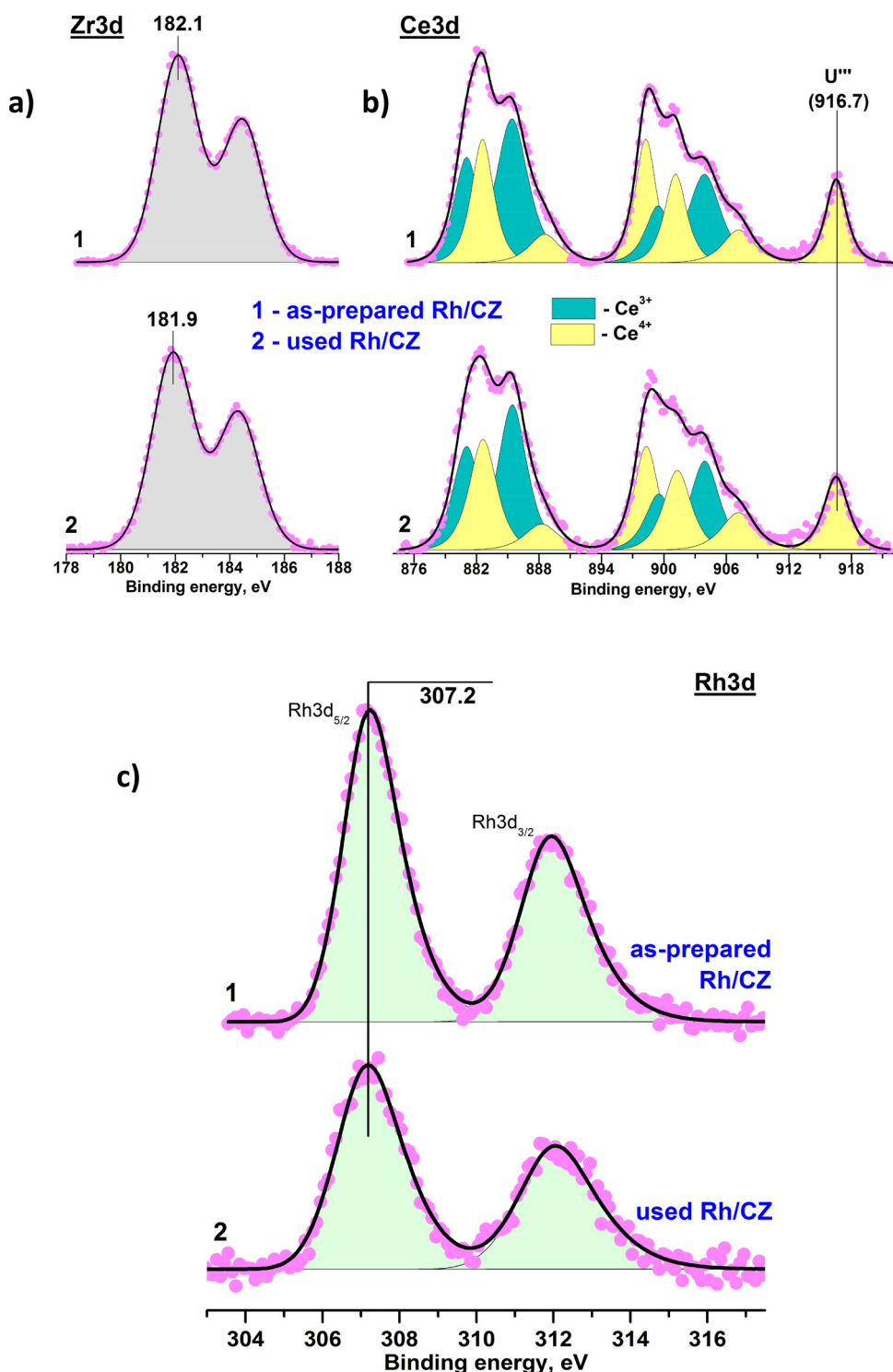


Fig. 2. XPS spectra of Zr3d (a), Ce3d (b) and Rh3d (c) of as-prepared and used in SD ATR 1 wt.% Rh/CZ.

3.3. Autothermal reforming of *n*-hexadecane and diesel fuel

Fig. 4 illustrates the effect of time on stream on the HD and SD conversion and gas product distribution for HD and SD ATR over Rh/CZ catalyst in a continuous-flow reactor. The experiment was started from HD ATR according to standard catalytic activity measurement procedure (Section 2.3); after 3 h of time on stream, HD was replaced by SD. One can see that the catalyst provided complete conversion of HD with product distribution close to the equilibrium composition. After change of HD by SD, the catalyst provided complete conversion of diesel for the

next 9 h. The conversion subsequently decreased from 100 to 86% during the next 6 h. Additionally, the outlet H₂ and CO concentrations decreased from 37 to 31 vol. %, and from 7 to 2 vol. %, respectively. The supplied oxygen converted completely during the entire duration of the experiment, the CO₂ concentration varied within 16–18 vol. %, that of CH₄ was about 1 vol. %, while the content of C₂–C₅ hydrocarbons was insignificant not exceeding 1 vol. %. The carbon deposit was insignificant and after annealing no agglomeration of Rh particles and no loss in the catalyst activity were observed.

Due to the exothermic character of SD ATR, carbon formation may

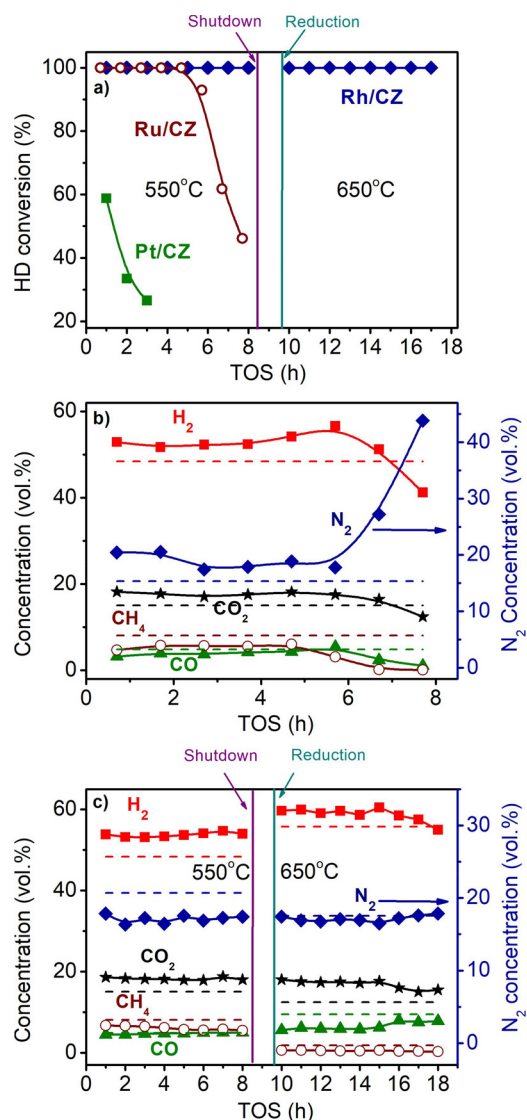


Fig. 3. The HD conversion (a) and product distribution on dry basis (b,c) over 1.9 wt.% Pt/CZ (a), 1 wt.% Ru/CZ (a,b) and 1 wt.% Rh/CZ (a,c) in the HD SR as a function of time on stream at $H_2O/C = 3.0$, $T = 550\text{--}650\text{ }^\circ\text{C}$ and $GHSV = 23,000\text{ h}^{-1}$. Points – experiment, dashed line – equilibrium.

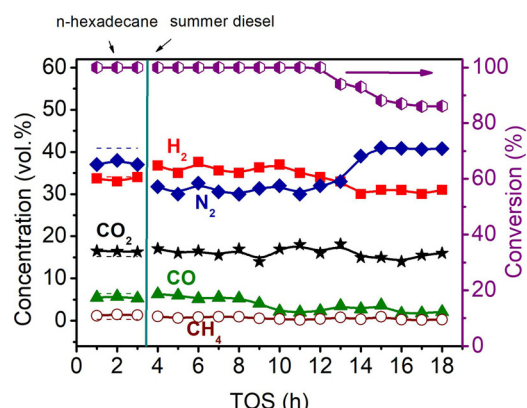


Fig. 4. The HD and SD conversion and product distribution on dry basis over 1 wt.% Rh/CZ in the HD ATR and SD ATR as a function of time on stream at $H_2O/C = 2.5$, $O_2/C = 0.5$, $T = 650\text{ }^\circ\text{C}$, $GHSV = 30,000\text{ h}^{-1}$. Points – experiment, dashed line – equilibrium.

be associated with possible hot spot formation at the frontal catalyst bed, which induces thermal cracking of diesel fuel components to form unsaturated hydrocarbons. To avoid this, the performance of the Rh/CZ catalyst can be strongly promoted by deposition onto carriers with high heat conductivity, such as metal foams and wire meshes. Preliminary results in this area with Rh/CZ were published recently [42] and more detailed research is ongoing. According to the literature [11,12,14,25], another opportunity to improve the catalyst performance consists of the increased Rh content up to 3–4 wt. % and reaction temperature.

3.4. Comparison with reported Rh-based catalysts

Several comparative surveys of different Rh-, Ru-, Pt-, and Ni-containing catalysts studied by various research teams in steam, auto-thermal reforming and partial oxidation of commercial diesel and diesel surrogate are available in literature [3–6]. However, direct comparison seems to be problematic owing to various reaction conditions used in different works. In particular, our results appeared to be comparable semi-quantitatively (See Table 2) with the data reported in Refs. [21,22], devoted to commercial diesel autothermal reforming over Rh- and Co, La, Mn promoted Rh-based monolithic catalysts which were the results of evolution of the earlier developments of the same research team [9–11,18,19]. Our results are also comparable with the data reported on *n*-hexadecane steam reforming over Rh/Al₂O₃ and Rh/CeO₂ [7,8] catalysts and diesel surrogate Norpar13 (ExxonMobil) steam reforming over Rh/CeO₂-Al₂O₃ [12] catalyst.

The authors of [21,22] studied ATR of low-sulfur diesel MK1 over 1 wt.% Rh and 6 wt.% X (X = Co, La or Mn) supported on CeO₂-ZrO₂. The process parameters at the experiments were as follows: O₂/C ~ 0.45, H₂O/C ~ 2.5 and GHSV ~ 50,000 h⁻¹. The RhCo catalyst was superior with fuel conversion of 95–99% in the temperature range of 700–950 °C. The RhLa and RhMn catalysts showed fuel conversion of 88–96 and 73–89%, respectively. The reference 3 wt.%Rh/CeO₂-ZrO₂ catalyst showed fuel conversion of 77–92% during ATR of commercial biodiesel (NExBTL, Neste Oil) under the same operational conditions. During time on stream experiments at 750 °C, all of these catalysts showed continuous decrease in both fuel conversion and H₂ yield. Based on the results of activity evaluation and characterization, the authors concluded that the lanthanum-promoted catalyst seemed to have the highest potential for diesel ATR. In our experiments under similar experimental conditions (O₂/C ~ 0.5, H₂O/C ~ 2.5 and GHSV ~ 30,000 h⁻¹), but at lower reaction temperature (650 °C), complete conversion of diesel was observed as well, and it also decreased with time. That is, similarly to the reported Rh-containing catalysts, the proposed Rh/CZ catalyst has sufficient activity and stability in diesel ATR.

In Ref. [7], steam reforming of *n*-hexadecane was studied over 21 wt. % Rh/Al₂O₃ and 12 wt. % Rh/CeO₂ supported on microstructured foils. At a temperature of 700 °C, H₂O/C = 4, GHSV = 50,000 h⁻¹, the maximum conversion of *n*-hexadecane on Rh/Al₂O₃ was 96%. However, the catalysts rapidly lost activity, and the conversion decreased to 65% in 12 h on stream. Rh/CeO₂ showed superior stability under the same conditions [7,8], and provided complete HD conversion after 15 h on stream. At a temperature of 645 °C, Rh/CeO₂ provided a HD conversion of 93% which decreased to 63% during 12 h on stream. Halving GHSV (to 25,000 h⁻¹) allowed a 100% HD conversion only at a temperature above 600 °C. In our experiments with Rh/CZ catalyst under similar experimental conditions (H₂O/C ~ 3 and GHSV ~ 23,000 h⁻¹), but at a lower reaction temperature (550 °C), complete conversion of *n*-hexadecane was observed during 8 h, and the catalyst showed stable operation during the next 5 h at 650 °C. That is, Rh/CZ seems to be more promising with respect to steam reforming of *n*-hexadecane, because Rh loading in this catalyst was more than one order of magnitude less than in Rh/Al₂O₃ and Rh/CeO₂ catalysts.

The authors of [12] studied steam reforming of diesel surrogate Norpar13 over 2 wt.% Rh/CeO₂-Al₂O₃ catalyst. It was found that at the

Table 2

Comparison of the Rh-based catalysts performance.

Catalyst	Type of Fuel	Reaction	Conditions					Conversion, %	$W_{H_2}^b$, mol g _{fuel} ⁻¹ min ⁻¹	Ref.
			GHSV, h ⁻¹	WHSV, h ⁻¹	H ₂ O/C	O ₂ /C	T, °C			
1wt.%Rh/CeO ₂ –ZrO ₂	Diesel Euro-5	ATR	30,000	29.5	2.5	0.5	650	100	0.27	This work
	<i>n</i> -hexadecane	SR	23,000	19.7	3		550	100	0.34	
1wt.%Rh + 6 wt.%Co/CeO ₂ –ZrO ₂	MK1	ATR	50,000		2.5	0.45	700–950	95–99		[21,22]
1wt.%Rh + 6 wt.%La/CeO ₂ –ZrO ₂	MK1	ATR	50,000		2.5	0.45	700–950	88–96		[21,22]
1wt.%Rh + 6 wt.%Mn/CeO ₂ –ZrO ₂	MK1	ATR	50,000		2.5	0.45	700–950	73–89		[21,22]
3wt.%Rh/CeO ₂ –ZrO ₂	NExBTL	ATR	50,000		2.5	0.45	700–950	77–92		[21,22]
21wt.%Rh/Al ₂ O ₃	<i>n</i> -hexadecane	SR	50,000		4		700	96 (65 ^a)		[7]
12wt.%Rh/CeO ₂	<i>n</i> -hexadecane	SR	50,000		4		700	100		[7,8]
		SR	50,000		4		645	93 (63 ^a)		[7,8]
		SR	25,000		4		600	100		[7,8]
2 wt.% Rh/CeO ₂ –Al ₂ O ₃	Norpar13	SR		5.1	3		550	100	0.13	[12]
		SR		5.1	3		800	100	0.18	[12]

^a Decreased in 12 h on stream.^b Hydrogen production rate per 1 g of catalyst.

inlet H₂O/C ~ 3 and feed weight hourly space velocity (WHSV) of 5.1 h⁻¹ (volumetric flow rates of 4.08 and 1.38 cm³/h of water and fuel, respectively, an approximately 1 g of catalyst were used in experiments), this catalyst showed stable operation during 55 h at 550 and 800 °C, with hydrogen production rates ~ 0.13 and 0.18 mol g_{fuel}⁻¹ min⁻¹, respectively.

In our experiments of *n*-hexadecane steam reforming with 1 wt.% Rh/CZ catalyst at WHSV = 19.7 h⁻¹, the hydrogen production rate per 1 g of catalyst at 550 °C was ~ 0.34 mol g_{fuel}⁻¹ min⁻¹. Taking into account twice lower Rh loading, the Rh/CZ catalyst has ~ 5 times higher hydrogen productivity per weight of noble metal. It is important to note also that the average velocity of carbon deposition defined as the ratio of total amount of detected carbon to the time of experiment was similar to that reported in [12].

These results suggest a conclusion that Rh/CZ catalyst demonstrated superior catalytic performance both in steam conversion and auto-thermal reforming of diesel. Therefore, further studies will be focused on evaluation of structured catalyst and investigation of catalytic performance in long run experiments.

4. Conclusions

Sorption-hydrolytic deposition technique enables production of highly dispersed catalysts based on noble metal (Pt, Ru, Rh) particles of 1–2 nm in size. The method is relatively easy to implement and has great potential for catalyst industry applications.

The prepared catalysts were tested in HD SR. Compared to Ru/CZ and Pt/CZ samples, the Rh/CZ catalyst was much more active and stable. Although the catalyst contained a small amount of supported Rh (1 wt.%), it provided complete HD SR for 17 h, HD and SD ATR for 12 h on stream at 650 °C. Comparative analysis of the obtained results and literature data corroborated superior catalytic performance and coking-resistance of Rh/CZ.

Acknowledgement

The authors appreciate the financial support from the Ministry of Education and Science of the Russian Federation, project No 14.607.21.0149, Unique Identification Number RFMEFI60716X0149.

Appendix A. Supplementary data

Supplementary material related to this article can be found, in the online version, at doi:<https://doi.org/10.1016/j.apcatb.2018.06.003>.

References

- X. Xu, P. Li, Y. Shen, Small-scale reforming of diesel and jet fuels to make hydrogen and syngas for fuel cells: a review, *Appl. Energy* 108 (2013) 202–217.
- A. Lindermeir, S. Kah, S. Kavurucu, M. Mühlner, On-board diesel fuel processing for an SOFC-APU-technical challenges for catalysis and reactor design, *Appl. Catal. B* 70 (2007) 488–497.
- S. Sengodan, R. Lan, J. Humphreys, D. Du, W. Xu, H. Wang, S. Tao, Advances in reforming and partial oxidation of hydrocarbons for hydrogen production and fuel cell applications, *Renew. Sustain. Energy Rev.* 82 (2018) 761–780.
- N. Abatzoglou, C. Fauteux-Lefebvre, Review of catalytic syngas production through steam or dry reforming and partial oxidation of studied liquid compounds, *Wiley Interdiscip. Rev. Energy Environ.* 5 (2016) 169–187.
- J. Bae, S. Lee, S. Kim, J. Oh, S. Choi, M. Bae, I. Kang, S.P. Katikaneni, Liquid fuel processing for hydrogen production: a review, *Int. J. Hydrogen Energy* 41 (2016) 19990–20022.
- R.M. Navarro Yerga, M.C. Álvarez-Galván, N. Mota, J.a. Villoria de la Mano, S.M. Al-Zahrani, J.L.G. Fierro, Catalysts for hydrogen production from heavy hydrocarbons, *ChemCatChem* 3 (2011) 440–457.
- J. Thormann, P. Pfeifer, U. Kunz, K. Schubert, Reforming of diesel fuel in a micro reactor, *Int. J. Chem. React. Eng.* 6 (2008) art. no. P1.
- J. Thormann, L. Maier, P. Pfeifer, U. Kunz, O. Deutschmann, K. Schubert, Steam reforming of hexadecane over a Rh/CeO₂ catalyst in microchannels: experimental and numerical investigation, *Int. J. Hydrogen Energy* 34 (2009) 5108–5120.
- A.V. González, X. Karatzas, L.J. Pettersson, Autothermal reforming of Fischer-Tropsch diesel over alumina and ceria-zirconia supported catalysts, *Fuel* 107 (2013) 162–169.
- X. Karatzas, D. Creaser, A. Grant, J. Dawody, L.J. Pettersson, Hydrogen generation from n-tetradecane, low-sulfur and Fischer-Tropsch diesel over Rh supported on alumina doped with ceria/lanthana, *Catal. Today* 164 (2011) 190–197.
- X. Karatzas, J. Dawody, A. Grant, E.E. Svensson, L.J. Pettersson, Zone-coated Rh-based monolithic catalyst for autothermal reforming of diesel, *Appl. Catal. B* 101 (2011) 226–238.
- C. Xie, Y. Chen, Y. Li, X. Wang, C. Song, Sulfur poisoning of CeO₂ – Al₂O₃ -supported mono- and bi-metallic Ni and Rh catalysts in steam reforming of liquid hydrocarbons at low and high temperatures, *Appl. Catal. A* 390 (2010) 210–218.
- S. Shah, O.G. Marin-Flores, K. Chinnathambi, M.G. Norton, S. Ha, Partial oxidation of surrogate jet-a fuel over SiO₂ supported MoO₃, *Appl. Catal. B* 193 (2016) 133–140.
- J.J. Spivey, Deactivation of reforming catalysts, in: D. Shekhatwati, J.J. Spivey, D.A. Berry (Eds.), *Fuel Cells: Technologies for Fuel Processing*, Elsevier, Amsterdam, 2011, pp. 285–315.
- S. Yoon, I. Kang, J. Bae, Effects of ethylene on carbon formation in diesel auto-thermal reforming, *Int. J. Hydrogen Energy* 33 (2008) 4780–4788.
- J.R. Rostrup-Nielsen, T. Christensen, I. Dybkjaer, Steam reforming of liquid hydrocarbons, *Recent Adv. Basic Appl. Ind. Catal.* 113 (1998) 81–95.
- J. Pasel, R.C. Samsons, A. Tschauder, R. Peters, D. Stolten, A novel reactor type for autothermal reforming of diesel fuel and kerosene, *Appl. Energy* 150 (2015) 176–184.
- J.A.J. Karlsson, P. Ekdunge, L. De Verdier, B. Ha, J. Dawody, M. Nilsson, L.J. Pettersson, Diesel fuel reformer for automotive fuel cell applications, *Int. J. Hydrogen Energy* 34 (2009) 3367–3381.
- X. Karatzas, M. Nilsson, J. Dawody, B. Lindström, L.J. Pettersson, Characterization and optimization of an autothermal diesel and jet fuel reformer for 5 kW mobile fuel cell applications, *Chem. Eng. J.* 156 (2010) 366–379.
- Y. Lu, J. Chen, Y. Liu, Q. Xue, M. He, Highly sulfur-tolerant Pt/Ce_{0.8}Gd_{0.2}O_{1.9} catalyst for steam reforming of liquid hydrocarbons in fuel cell applications, *J. Catal.* 254 (2008) 39–48.
- M.Z. Granlund, K. Jansson, M. Nilsson, J. Dawody, L.J. Pettersson, Evaluation of Co, La, and Mn promoted Rh catalysts for autothermal reforming of commercial diesel:

aging and characterization, *Appl. Catal. B* 172–173 (2015) 145–153.

[22] M.Z. Granlund, K. Jansson, M. Nilsson, J. Dawody, L.J. Pettersson, Evaluation of Co, La, and Mn promoted Rh catalysts for autothermal reforming of commercial diesel, *Appl. Catal. B* 154 (2014) 386–394.

[23] N. Mota, M.C. Alvarez-Galvan, J.A. Villoria, F. Rosa, J.L.G. Fierro, R.M. Navarro, Reforming of diesel fuel for hydrogen production over catalysts derived from $\text{LaCo}_{1-x}\text{M}_x\text{O}_3$ ($\text{M}=\text{Ru}, \text{Fe}$), *Top. Catal.* 3 (2009) 1995–2000.

[24] M.C. Alvarez-Galvan, R.M. Navarro, F. Rosa, Y. Bricen, F.G. Alvarez, J.L.G. Fierro, Performance of La, Ce-modified alumina-supported Pt and Ni catalysts for the oxidative reforming of diesel hydrocarbons, *Int. J. Hydrogen Energy* 33 (2008) 652–663.

[25] Q. Zheng, C. Janke, R. Farrauto, Steam reforming of sulfur-containing dodecane on a Rh – Pt catalyst: influence of process parameters on catalyst stability and coke structure, *Appl. Catal. B* 160–161 (2014) 525–533.

[26] D.J. Haynes, D.A. Berry, D. Shekhawat, J.J. Spivey, Catalytic partial oxidation of n-tetradecane using pyrochlores: effect of Rh and Sr substitution, *Catal. Today* 136 (2008) 206–213.

[27] X. Karatzas, K. Jansson, J. Dawody, R. Lanza, L.J. Pettersson, Microemulsion and incipient wetness prepared Rh-based catalyst for diesel reforming, *Catal. Today* 175 (2011) 515–523.

[28] E.A. Alikin, S.P. Denisov, N.M. Danchenko, V.N. Rychkov, A.S. Volkov, A.S. Karpov, Thermally stable composite system $\text{Al}_2\text{O}_3 - \text{Ce}_{0.75}\text{Zr}_{0.25}\text{O}_2$ for automotive three way catalysts, *Catal. Ind.* 5 (2013) 133–142.

[29] P.A. Simonov, T.B. Shoynkhorova, P.V. Snytnikov, D.I. Potemkin, V.D. Belyaev, V. A. Sobyanin, Method of Catalyst Preparation, Russian Patent Application №2017122244 from 26.06.2017, 2017.

[30] L. Wu, B.E. Schwederski, D.W. Margerum, Stepwise hydrolysis kinetics of tetra-chloroplatinate(II) in base, *Inorg. Chem.* 29 (1990) 3578–3584.

[31] D. Kashchiev, G.M. van Rosmalen, Review: nucleation in solutions revisited, *Cryst. Res. Technol.* 38 (2003) 555–574.

[32] J. Freel, Chemisorption on supported platinum, *J. Catal.* 25 (1972) 139–148.

[33] R.J. Madon, E. Iglesia, Catalytic reaction rate in thermodynamically non-ideal systems, *J. Mol. Catal. A* 163 (2000) 189–204.

[34] D.A. Svintsitskiy, T.Y. Kardash, E.M. Slavinskaya, O.A. Stonkus, S.V. Koscheev, A.I. Boronin, The decomposition of mixed oxide $\text{Ag}_2\text{Cu}_2\text{O}_3$: structural features and the catalytic properties in CO and C_2H_4 oxidation, *Appl. Surf. Sci.* 427 (2018) 363–374.

[35] D.A. Svintsitskiy, E.M. Slavinskaya, T.Y. Kardash, V.I. Avdeev, B.V. Senkovskiy, General low-temperature catalytic CO oxidation over mixed silver – copper, *Appl. Catal. A* 510 (2016) 64–73.

[36] J.F. Moulder, W.F. Stickle, P.E. Sobol, K.D. Bomben, *Handbook of X-Ray Photoelectron Spectroscopy*, Perkin-Elmer Corp, Eden Prairie, Minnesota, USA, 1992.

[37] A.V. Naumkin, A. Kraut-Vass, S.W. Gaarenstroom, C.J. Powell, NIST X-Ray Photoelectron Spectroscopy (XPS) Database, Version 3.5, (2012) <https://srdata.nist.gov/xps/>.

[38] L.S. Kibis, A.I. Stadnichenko, S.V. Koscheev, V.I. Zaikovskii, A.I. Boronin, XPS study of nanostructured rhodium oxide film comprising Rh^{4+} species, *J. Phys. Chem. C* 120 (2016) 19142–19150.

[39] P. Fornasiero, R. Dimonte, G.R.R. Rao, J. Kaspar, S. Meriani, A. Trovarelli, M. Graziani, Rh-loaded $\text{CeO}_2\text{-ZrO}_2$ solid-solutions as highly efficient oxygen exchangers: dependence of the reduction behavior and the oxygen storage capacity on the structural-properties, *J. Catal.* 151 (1995) 168–177.

[40] G. Jones, J.G. Jakobsen, S.S. Shim, J. Kleis, M.P. Andersson, J. Rossmeisl, F. Abild-Pedersen, T. Bligaard, S. Helveg, B. Hinnemann, J.R. Rostrup-Nielsen, I. Chorkendorff, J. Sehested, J.K. Nørskov, First principles calculations and experimental insight into methane steam reforming over transition metal catalysts, *J. Catal.* 259 (2008) 147–160.

[41] J.R. Rostrup-Nielsen, Activity of nickel catalysts for steam of hydrocarbons, *J. Catal.* 31 (1973) 173–199.

[42] T.B. Shoynkhorova, V.N. Rogozhnikov, P.A. Simonov, P.V. Snytnikov, A.N. Salanov, A.V. Kulikov, E.Y. Gerasimov, V.D. Belyaev, D.I. Potemkin, V.A. Sobyanin, Highly dispersed $\text{Rh}/\text{Ce}_{0.75}\text{Zr}_{0.25}\text{O}_{2.8-\eta}\text{-Al}_2\text{O}_3/\text{FeCrAl}$ wire mesh catalyst for autothermal n-hexadecane reforming, *Mater. Lett.* 214 (2018) 290–292.